Comparison of Different Spectral Domain OCT Scanning Protocols for Diagnosing Preperimetric Glaucoma

Renato Lisboa,[1,2] Augusto Paranhos Jr,[2] Robert N. Weinreb,[1] Linda M. Zangwill,[1] Mauro T. Leite,[2] and Felipe A. Medeiros[1]

[1]Hamilton Glaucoma Center, Department of Ophthalmology, University of California-San Diego, La Jolla, California
[2]Department of Ophthalmology, Federal University of São Paulo, São Paulo, Brazil

Correspondence: Felipe A. Medeiros, Hamilton Glaucoma Center, University of California-San Diego, 9500 Gilman Drive, La Jolla, CA 92093; fmedeiros@glaucoma.ucsd.edu.

Submitted: January 17, 2013
Accepted: March 12, 2013

Citation: Lisboa R, Paranhos A Jr, Weinreb RN, Zangwill LM, Leite MT, Medeiros FA. Comparison of different spectral domain OCT scanning protocols for diagnosing preperimetric glaucoma. *Invest Ophthalmol Vis Sci*. 2013;54:3417–3425. DOI:10.1167/iovs.13-11676

Purpose. To compare the ability of spectral-domain optical coherence tomography (SDOCT) retinal nerve fiber layer (RNFL), optic nerve head (ONH), and macular measurements to detect preperimetric glaucomatous damage.

Methods. The study included 142 eyes from 91 patients suspected of having the disease based on the appearance of the optic disc. All eyes had normal visual fields before the imaging session. Forty-eight eyes with progressive glaucomatous damage were included in the preperimetric glaucoma group. Ninety-four eyes without any evidence of progressive glaucomatous damage and followed untreated for 12.8 ± 3.6 years were used as controls. Areas under the receiver operating characteristic curves (AUC) were calculated to summarize diagnostic accuracies of the parameters.

Results. The three RNFL parameters with the largest AUCs were average RNFL thickness (0.89 ± 0.03), inferior hemisphere average thickness (0.87 ± 0.03), and inferior quadrant average thickness (0.85 ± 0.03). The three ONH parameters with the largest AUCs were vertical cup-to-disc ratio (0.74 ± 0.04), rim area (0.72 ± 0.05), and rim volume (0.72 ± 0.05). The three macular parameters with the largest AUCs were GCC average thickness (0.79 ± 0.04), GCC inferior thickness (0.79 ± 0.05), and GCC superior thickness (0.76 ± 0.05). Average RNFL thickness performed better than vertical cup-to-disc ratio (0.89 vs. 0.74; $P = 0.007$) and GCC average thickness (0.89 vs. 0.79; $P = 0.015$).

Conclusions. SDOCT RNFL measurements performed better than ONH and macular measurements for detecting preperimetric glaucomatous damage in a cohort of glaucoma suspects. (ClinicalTrials.gov number, NCT00221897.)

Keywords: preperimetric, glaucoma, diagnosis

Structural assessment of the optic nerve is an essential component of glaucoma diagnosis and management.[1–4] The use of spectral-domain optical coherence tomography (SDOCT) technology has enabled clinicians to obtain unprecedented high-resolution images of the optic nerve head (ONH) and retinal nerve fiber layer (RNFL) structures in a fraction of the time required by previous technologies. SDOCT is also able to image the macular area, where the highest concentration of ganglion cells is found, and macular imaging has been proposed as a useful tool for structural assessment of glaucomatous damage.[5]

Several previous studies have evaluated the accuracies of RNFL, ONH, and macula scans provided by SDOCT for glaucoma diagnosis.[6–10] Although these studies are important in providing an initial assessment and comparison of these scanning areas, their estimates of diagnostic accuracy might not directly correspond to the performance of these tests when used in clinical practice. In these studies, diagnostic accuracy was assessed based on the ability to differentiate patients with clearly defined glaucomatous visual field damage from healthy eyes without any suspicious findings for the disease. However, in clinical practice, one is interested in the ability of the diagnostic test in evaluating the presence of disease in those suspected of a condition, not in those with clearly defined diagnoses. Therefore, to justify the cost and expense of applying an additional diagnostic test for glaucoma evaluation, it is important to demonstrate its benefit in providing additional clinical information besides what can be gathered from the conventional clinical examination and visual field assessment. In the absence of clearly defined visual field losses, SDOCT could potentially be used to differentiate eyes with preperimetric glaucomatous damage from eyes that show suspicious optic disc appearances, but no structural damage.

The purpose of this study was to evaluate and compare the accuracies of SDOCT assessment of RNFL, ONH, and macular areas for diagnosing preperimetric glaucoma in a cohort of patients suspected of having the disease. Documented longitudinal assessment of the optic nerve was used as the reference standard to establish the final diagnosis of preperimetric damage and allow comparison of the accuracies of the different scanning areas.[11–15]

Methods

Participants

This was an observational cohort study that included patients recruited from the Diagnostic Innovations in Glaucoma Study (DIGS) conducted at the Hamilton Glaucoma Center (University

Copyright 2013 The Association for Research in Vision and Ophthalmology, Inc.

Downloaded from iovs.arvojournals.org on 03/01/2021

of California-San Diego). Participants were longitudinally evaluated according to an established protocol that included visits with complete clinical examination and several imaging and functional tests. All participants who met the inclusion criteria described below were enrolled and all data were entered in a computer database. Informed consent was obtained from all participants. The University of California-San Diego Human Subjects Committee approved all protocols, and methods described adhered to the tenets of the Declaration of Helsinki.

Each subject underwent a comprehensive ophthalmic examination, including review of medical history, best corrected visual acuity, slit-lamp biomicroscopy, IOP measurement using Goldmann applanation tonometry, gonioscopy, dilated fundoscopic examination using a 78-diopter (D) lens, stereoscopic optic disc photography, and standard automated perimetry (SAP) with 24-2 Swedish Interactive Threshold Algorithm (Carl Zeiss Meditec, Inc., Dublin, CA).

To be included, subjects had to have best-corrected visual acuity of 20/40 or better, spherical refraction within ±5.0 D, cylinder correction within 3.0 D, and open angle with gonioscopy. Subjects with coexisting retinal disease, uveitis, or nonglaucomatous optic disc neuropathy were excluded from the study.

A cohort of participants suspected of having glaucoma was selected from our database. These participants were initially selected based on the presence of suspicious appearance of the optic nerve from cross-sectional evaluation of stereophotographs at the time of imaging by two independent masked graders. A third grader reviewed the stereophotographs in case of disagreement. Features characteristic of suspicious glaucomatous appearance of the optic disc were neuroretinal rim narrowing, cupping, or suspicious RNFL defects. All participants had a normal SAP visual field result at the time of imaging. A normal visual field was defined as a mean deviation and pattern standard deviation within 95% confidence limits and a glaucoma hemifield test result within normal limits. Additionally, participants did not have repeatable glaucomatous visual field loss before the date of their examination with imaging instruments. All participants had been previously followed for at least 5 years before their imaging session.

These participants were then classified into cases and controls based on history of documented evidence of progressive glaucomatous change in the appearance of the optic disc occurring *before* the imaging sessions. Patients with documented evidence of progressive glaucomatous nerve damage at any time before both imaging sessions with SDOCT were considered as having preperimetric glaucoma. That is, preperimetric glaucoma was defined based on the presence of documented evidence of progressive structural damage to the optic nerve in the absence of visual field loss on SAP. Progressive glaucomatous change in the appearance of the optic disc was assessed by simultaneous stereophotographs (TRC-SS; Topcon Instrument Corp. of America, Paramus, NJ). Stereophotographic sets of slides were examined using a stereoscopic viewer (Asahi; Pentax, Tokyo, Japan). The stereophotographs were evaluated by two experienced graders, and each was masked to the subject's identity, to other test results, and to the chronological sequence of the stereophotographs. For inclusion, stereophotographs needed to be graded adequate or better. Definition of change was based on focal or diffuse narrowing of the neuroretinal rim, increased excavation, or enlargement of the RNFL defects. Changes on rim color, presence of disc hemorrhages, or progressive peripapillary atrophy were not sufficient for characterization of progression. Discrepancies between the two graders were resolved by either consensus or adjudication of a third experienced grader.

A total of 48 eyes from 42 participants with progressive optic disc damage and no visual field loss were included in the preperimetric glaucoma group. These subjects were followed for an average of 13.6 ± 4.2 years.

Patients without any evidence of progressive change in the appearance of the optic disc and without any evidence of visual field loss in both eyes were used as controls. Control eyes were also required to have no history of treatment during follow-up in order to avoid a confounding effect of treatment in preventing the development of progressive disc damage. A total of 94 eyes from 49 patients were included as a control group. These subjects had been followed untreated for an average of 12.8 ± 3.6 years without showing any evidence of progressive damage to the optic nerve.

Instrumentation

RTVue (software version 6.1.0.4; Optovue, Inc., Fremont, CA) was used to obtain SDOCT scans. RTVue uses a superluminescent diode scan with a center wavelength of 840 nm to provide high-resolution images. The instrument is able to collect 26,000 A-scans per second with an axial resolution of 5 μm. The ONH protocol and ganglion cell complex (GCC) protocol were used in this study. All patients had both protocols performed within 6 months of each other.

Peripapillary Retinal Nerve Fiber Layer Measurements. The ONH protocol was used to obtain RNFL measurements. This protocol generates an RNFL thickness map measured along a circle of 3.45 mm in diameter centered at the ONH. After the RNFL map is obtained, the RNFL thickness parameters are estimated by assessing a total of 2325 data points between the anterior and posterior RNFL borders. Several subdivisions of the entire measurement circle are performed. First, the overall average, together with the superior hemisphere, inferior hemisphere, temporal quadrant, superior quadrant, nasal quadrant, and inferior quadrant are provided. Then, each quadrant is divided in two, generating eight sectors of 45°. Finally, each 45° sector is divided into two more sectors, generating 16 sectors of 22.5°. Only good-quality images, as defined by a signal strength index greater than or equal to 28, were included in the analyses.

Optic Nerve Head Measurements. The ONH protocol was used to obtain ONH measurements. It consists of 12 radial scans of 3.4 mm in length (455 A-scans each) and 13 concentric circular scans ranging from 1.3 to 4.9 mm in diameter (425–965 A-scans each) and centered at the ONH. This protocol provides 14,141 A-scans in 0.55 seconds. Areas between the scans are interpolated. All images were processed with three-dimensional/video baseline. Although the delineation of the optic disc margin is automated, all images were reviewed. When necessary, images were manually delineated and centered at the optic disc by identifying and joining the RPE tips. The RTVue software (software version 6.1.0.4; Optovue, Inc.) automatically defines the optic cup as the intersection of the nerve head inner boundary and a parallel line that is 150 μm above the connecting line of the RPE tips. The ONH parameters measured by the software were rim area, rim volume, vertical cup-to-disc ratio, horizontal cup-to-disc ratio, cup area, cup volume, cup-to-disc area ratio, disc area, and nerve head volume. Only good-quality images, as defined by a signal strength index greater than or equal to 28, were included in the analyses.

Macular Measurements. The GCC protocol was used to obtain macular measurements. This protocol consists of one horizontal line scan of 7 mm in length (467 A-scans) followed by 15 vertical line scans of 7 mm in length (400 A-scans each) at 0.55-mm intervals. This protocol provides 14,810 A-scans in 0.58 seconds of a rectangular area. However, the area analyzed

Investigative Ophthalmology & Visual Science

Downloaded from iovs.arvojournals.org on 03/01/2021

by the software (RTVue, software version 6.1.0.4; Optovue, Inc.) involves a 6-mm-diameter circle inside the rectangular area scanned by the instrument. The analyzed circular area is centered 1 mm temporal to the fovea. This slight offset provides a more temporal retina analysis, which corresponds to the nasal visual field where glaucomatous damage is most likely to occur at initial stages of the disease (e.g., nasal step). The GCC protocol provides a segmentation of macular B-scans in two layers: GCC layer and outer retinal layer. The GCC layer is composed of the ganglion cell layer, the nerve fiber layer, and the inner plexiform layer. The GCC layer parameters generated by the GCC protocol are average thickness, superior thickness, inferior thickness, superior minus inferior thickness, global loss volume (GLV), focal loss volume (FLV), and root mean square (RMS). The calculations for GLV, FLV, and RMS have been described in detail elsewhere.[6] Briefly, GLV measures the average amount of GCC loss over the entire GCC map, whereas FLV measures the average amount of focal GCC loss over the entire GCC map. GLV best detects diffuse ganglion cell loss, similar to mean deviation in visual fields. Likewise, FLV best detects local ganglion cell loss using a pattern deviation map to correct for overall absolute changes, similar to pattern standard deviation in visual fields. The RMS or pattern coefficient of variation provides a summary of how well the fractional map (used to calculate the GLV) and pattern deviation map (used to calculate the FLV) of an individual fit the normal pattern. The worse the fit, the greater the value.

In addition to GCC layer parameters, the GCC protocol also evaluates the full retina and outer retina, separately. The parameters provided for each of them are average thickness, superior thickness, inferior thickness, and superior minus inferior thickness.

Only images acquired within 6 months of the ONH protocol and with good quality, as defined by a signal strength index greater than or equal to 32, were included in the analyses.

Statistical Analysis

Descriptive statistics included mean and SD for normally distributed variables and mean, first quartile, median, and third quartile for non-normally distributed variables.

To evaluate the ability of the parameters to differentiate between controls and preperimetric glaucomatous eyes, areas under the receiver operating characteristic (ROC) curves (AUC) were calculated. An AUC equal to 1 represents perfect discrimination, whereas an AUC of 0.5 represents chance discrimination. Sensitivity at fixed specificities of 80% and 95% were also reported for each parameter. AUCs were adjusted for sex differences between groups using the covariate adjusting procedure proposed by Pepe et al.[16] Pairwise comparisons of the AUCs were performed between the best parameters of each protocol.[16] A bootstrap resampling procedure ($n = 1000$ resamples) was used to derive the confidence intervals.[17] To account for potential correlation between eyes, the cluster of the data for the study subject was considered as the unit of resampling when calculating SEs. This procedure has been used to adjust for the presence of multiple correlated measurements of the same unit.[17,18]

All statistical analyses were performed with commercially available software (Stata version 11; Stata Corp., College Station, TX). The alpha level (type I error) was set at 0.05.

Results

Table 1 shows demographic and clinical characteristics of the eyes included in the study. No differences in age and ancestry were found between groups. There were more male subjects in the preperimetric glaucoma group than in the control group. Therefore, all ROC curves and comparisons were adjusted for sex differences between groups. Forty eyes included in the preperimetric group presented rim changes, whereas eight eyes presented changes on both RNFL and rim.

Peripapillary Retinal Nerve Fiber Layer Measurements

Table 2 shows mean values of RNFL parameters in the preperimetric glaucoma and control groups. Preperimetric glaucomatous eyes had, on average, significantly thinner RNFL measurements than control eyes. The three RNFL parameters with largest AUCs were average thickness (0.89 ± 0.03), inferior hemisphere average RNFL thickness (0.87 ± 0.03), and inferior quadrant RNFL thickness (0.85 ± 0.03). Pairwise comparisons did not demonstrate statistically significant differences between the AUCs of these parameters ($P > 0.05$ for all comparisons). The parameter with the highest sensitivity at fixed specificity of 95% was average thickness (70.8%). Figure 1 shows the ROC curves of the three RNFL parameters with largest AUCs.

Optic Nerve Head Measurements

Table 3 shows mean values of ONH parameters in the preperimetric glaucoma and control groups. Statistically significant differences were found for all parameters, except for disc area. The 3 ONH parameters with largest AUCs were vertical cup-to-disc ratio (0.74 ± 0.04), rim area (0.72 ± 0.05), and rim volume (0.72 ± 0.05). Pairwise comparisons did not show statistically significant differences between AUCs of these parameters ($P > 0.05$ for all comparisons). Rim area, rim volume, nerve head volume, and cup-to-disc area ratio showed the same sensitivity of 27.1% at fixed specificity of 95%. Figure 2 shows the ROC curves for the three ONH parameters with largest AUCs.

Macular Measurements

Table 4 shows mean values of macular parameters in the preperimetric glaucoma and control groups. Statistically significant differences were found for all GCC parameters, except for superior minus inferior GCC thickness. Statistically significant differences were also found for all full retinal parameters, except for superior minus inferior full retinal thickness. No statistically significant differences were found for outer retinal parameters. The three macular parameters with largest AUCs were GCC average thickness (0.79 ± 0.04), GCC inferior thickness (0.79 ± 0.05), and GCC superior thickness (0.76 ± 0.05). Pairwise comparisons did not show statistically significant differences between the AUCs of these parameters ($P > 0.05$ for all comparisons). The best GCC parameter, GCC average thickness, performed better than the best full retinal parameter, inferior full retinal thickness (0.79 vs. 0.70; $P = 0.009$), and the best outer retinal parameter, superior minus inferior outer retinal thickness (0.79 vs. 0.58; $P = 0.002$). The parameter with higher sensitivity at fixed specificity of 95% was GCC average thickness (43.8%). Figure 3 shows the ROC curves of the three macular parameters with largest AUCs.

Comparison of RNFL, ONH, and Macular Measurements

The RNFL parameter with largest AUC, average RNFL thickness, performed significantly better than the macular parameter with largest AUC, GCC average thickness (0.89 vs.

Investigative Ophthalmology & Visual Science

Downloaded from iovs.arvojournals.org on 03/01/2021

Table 1. Demographic and Clinical Characteristics of the Preperimetric Glaucoma and Control Study Groups

Characteristics	Preperimetric Glaucoma, $n = 48$	Control, $n = 94$	P Value
Age, y	65.9 ± 9.1	64.2 ± 11.2	0.427
% male	52.4	30.6	0.035
% African American	16.7	4.1	0.108
MD, dB	−0.81 (−1.82, −0.80, 0.12)	0.02 (−0.64, 0.25, 0.83)	0.001
PSD, dB	1.75 (1.46, 1.70, 1.84)	1.63 (1.29, 1.58, 1.81)	0.049
Follow-up, y	13.6 ± 4.2	12.8 ± 3.6	0.297

MD, mean deviation; PSD, pattern standard deviation.

0.79; $P = 0.007$), for differentiating between the preperimetric glaucoma and control groups. The average RNFL thickness also performed significantly better than the ONH parameter with largest AUC, vertical cup-to-disc ratio (0.89 vs. 0.74; $P = 0.015$). No statistically significant difference was found between vertical cup-to-disc ratio and GCC inferior thickness (0.79 vs. 0.74; $P = 0.46$). Figure 4 shows the ROC curves for the parameters with largest AUCs of each protocol.

Discussion

In the present study, we demonstrated that SDOCT RNFL assessment with the RTVue performed significantly better than ONH and macular assessments with the same instrument for detection of preperimetric glaucoma. To our knowledge, this is the first study that evaluated and compared the diagnostic accuracies of these measurements for detection of preperi-

Table 2. Mean ± SD Values of Peripapillary RNFL Thickness With AUC Curves and Sensitivities at Fixed Specificities for Discriminating Between Preperimetric Glaucoma and Control Groups

RNFL Thickness Parameter	Preperimetric Glaucoma, $n = 48$	Control, $n = 94$	P Value*	AUC (SE)	Sensitivity at 95% Specificity, %	Sensitivity at 80% Specificity, %
Average and quadrants						
Average	86.0 ± 7.6	99.5 ± 8.2	<0.001	0.89 (0.03)	70.8	79.2
Inferior hemisphere	85.7 ± 8.3	100.1 ± 9.0	<0.001	0.87 (0.03)	64.6	75.0
Inferior quadrant	104.9 ± 12.1	124.5 ± 13.5	<0.001	0.85 (0.03)	50.0	75.0
Superior hemisphere	86.3 ± 8.7	98.8 ± 9.4	<0.001	0.83 (0.03)	47.9	77.1
Superior quadrant	100.4 ± 11.0	116.0 ± 13.8	<0.001	0.81 (0.04)	43.8	53.2
Nasal quadrant	69.2 ± 11.5	78.6 ± 8.5	<0.001	0.75 (0.04)	45.8	58.3
Temporal quadrant	69.6 ± 9.8	78.7 ± 10.3	<0.001	0.73 (0.04)	29.2	45.8
45° sectors						
IT	111.4 ± 18.1	136.4 ± 17.2	<0.001	0.83 (0.03)	43.8	68.8
ST	106.7 ± 14.5	127.5 ± 16.8	<0.001	0.81 (0.03)	45.8	68.8
NU	73.2 ± 12.0	82.8 ± 9.9	<0.001	0.74 (0.04)	33.3	62.5
NL	65.2 ± 12.3	74.4 ± 9.0	<0.001	0.73 (0.04)	43.8	52.1
IN	98.5 ± 14.4	112.6 ± 18.6	<0.001	0.72 (0.04)	20.8	52.1
TU	71.3 ± 10.8	80.4 ± 11.5	<0.001	0.72 (0.04)	16.7	52.1
TL	67.9 ± 10.7	77.0 ± 11.8	<0.001	0.71 (0.04)	22.9	37.5
SN	94.1 ± 14.3	104.6 ± 14.5	<0.001	0.70 (0.04)	33.3	54.2
22.5° sectors						
IT1	119.6 ± 18.4	145.4 ± 18.9	<0.001	0.82 (0.03)	41.7	64.6
ST2	105.0 ± 19.0	129.2 ± 18.7	<0.001	0.81 (0.04)	41.7	64.6
TU2	77.6 ± 11.9	91.3 ± 14.7	<0.001	0.77 (0.04)	39.6	60.4
IT2	103.1 ± 22.3	127.4 ± 23.0	<0.001	0.77 (0.04)	31.9	60.4
NU1	64.1 ± 11.1	72.6 ± 8.1	<0.001	0.74 (0.05)	39.6	62.5
NU2	82.2 ± 14.4	93.0 ± 13.7	<0.001	0.73 (0.04)	27.1	58.3
NL2	69.2 ± 14.2	79.0 ± 11.0	<0.001	0.73 (0.04)	20.8	54.2
NL1	61.2 ± 11.7	69.8 ± 8.7	<0.001	0.72 (0.05)	33.3	52.1
TL2	72.5 ± 12.3	84.6 ± 15.9	<0.001	0.72 (0.04)	25.0	45.8
ST1	108.4 ± 17.2	125.7 ± 22.8	<0.001	0.72 (0.04)	12.5	43.8
IN1	104.8 ± 17.2	121.5 ± 22.4	<0.001	0.71 (0.04)	14.6	50.0
SN2	96.5 ± 15.4	107.3 ± 15.8	0.001	0.69 (0.05)	25.0	43.8
SN1	91.8 ± 16.1	101.9 ± 16.2	0.002	0.68 (0.05)	27.1	54.2
IN2	92.1 ± 14.2	103.6 ± 17.2	<0.001	0.68 (0.05)	23.4	39.6
TL1	63.3 ± 10.9	69.4 ± 10.9	0.003	0.65 (0.05)	18.8	39.6
TU1	65.0 ± 11.6	69.5 ± 10.9	0.035	0.59 (0.05)	22.9	25.0

IT, inferotemporal; ST, superotemporal; NL, lower nasal; NU, upper nasal; IN, inferonasal; SN, superonasal; TL, lower temporal; TU, upper temporal.

* For comparison of mean values of peripapillary retinal nerve fiber layer parameters between preperimetric glaucoma and control groups.

Investigative Ophthalmology & Visual Science

Downloaded from iovs.arvojournals.org on 03/01/2021

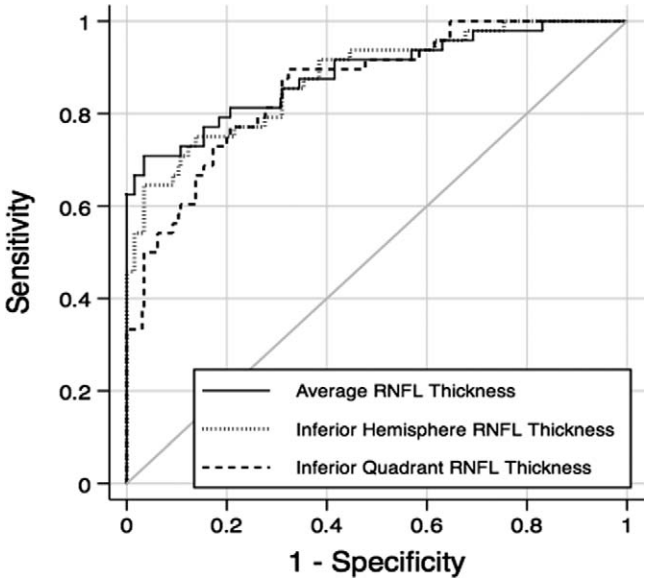

FIGURE 1. ROC curves for the three RNFL parameters with largest areas under the ROC curves: average RNFL thickness, inferior hemisphere RNFL thickness, and inferior quadrant RNFL thickness.

metric damage in a cohort of patients suspected of having glaucoma.

Several previous studies have evaluated the performance of SDOCT to detect glaucomatous damage.[6–10] Most of these studies have used visual field loss as the reference standard for classifying eyes as glaucomatous. That is, patients in these studies have been primarily selected based on the presence of clearly defined repeatable glaucomatous visual field loss, whereas controls were subjects without visual field damage or other suspicious findings for the disease. These studies are important for an initial evaluation of an instrument that is being considered as a potential diagnostic tool. In other words, if the instrument fails to differentiate patients with clearly defined disease versus those without any suspicious findings of damage, it will generally be considered inappropriate for diagnostic purposes. However, if the test succeeds at this stage, further steps are necessary in order to evaluate its capacity to provide relevant information that could be helpful in real clinical scenarios. Ancillary tests are used when there is diagnostic uncertainty, that is, in patients who are suspected of having the disease, not in those with clearly established diagnoses. In fact, in the absence of diagnostic uncertainty, no further diagnostic testing should be necessary. The presence of repeatable glaucomatous visual field damage obviates the need for performing a potentially costly imaging evaluation for diagnosing the disease, as the diagnosis will be already clear. To assess the potential of imaging devices as ancillary diagnostic tests, one needs to evaluate their performance in the presence of diagnostic uncertainty. We included a cohort of patients suspected of having glaucoma in our study and it should be noted that, at the time of imaging assessment, cases and controls were indistinguishable based on results of commonly performed clinical examinations, such as clinical optic disc evaluation and visual field assessment. This situation characterizes the presence of diagnostic uncertainty and the need for an additional test to assist in clarifying the diagnosis. By applying this design, the estimates of accuracy provided in our study are more likely to correspond to the real performance of imaging tests when used to diagnose glaucoma in clinical practice, compared with estimates of accuracy provided by previous studies.[6–10]

The AUCs reported in our study were considerably lower than the ones reported in previous studies that evaluated the diagnostic ability of SDOCT in glaucoma.[6–10] That can be explained by the less advanced stage of the disease of eyes included in the preperimetric glaucomatous group. In addition, the decreased performance is also related to the selection criteria of the control eyes, which had suspicious appearance of the optic disc. In a recent study by Rao et al.,[19] the ability of most SDOCT parameters in detecting glaucoma decreased significantly when evaluated against a clinically relevant control group that had suspicious appearance of the optic disc. The inclusion criteria used in our study selected a more homogeneous cohort, making it more difficult for the imaging test to differentiate similar groups frequently found in the clinical practice.

RNFL measurements performed significantly better than optic disc measurements in our study. This finding indicates that in the presence of suspicious optic disc appearance, RNFL assessment seems to be more useful than optic disc topographic measurements to establish the diagnosis. This may be directly related to the way that patients are identified as suspected of having glaucoma. As the evaluation of RNFL integrity during clinical examination or in stereophotographs is frequently difficult, most of these eyes are identified as suspects because of the presence of suspicious rim narrowing or enlarged optic disc cups. In this situation, it is not surprising that RNFL assessment provides more additional information for establishing the definitive diagnosis than further evaluation of optic disc rim and cup features by topographic parameters. It should be noted that the way eyes were identified as suspects for inclusion in our study resembles the way they are identified

TABLE 3. Mean ± SD Values of ONH With AUC Curves and Sensitivities at Fixed Specificities for Discriminating Between Preperimetric Glaucoma and Control Groups

ONH Parameter	Preperimetric Glaucoma, $n = 48$	Control, $n = 94$	*P* Value*	AUC (SE)	Sensitivity at 95% Specificity, %	Sensitivity at 80% Specificity, %
Vertical cup-to-disc ratio	0.79 ± 0.15	0.66 ± 0.19	0.001	0.74 (0.04)	18.8	56.3
Rim area, mm^2	0.66 ± 0.31	0.93 ± 0.32	<0.001	0.72 (0.05)	27.1	52.1
Rim volume, mm^3	0.06 ± 0.06	0.11 ± 0.09	0.001	0.72 (0.05)	27.1	52.1
Nerve head volume, mm^3	0.12 ± 0.10	0.21 ± 0.14	0.001	0.72 (0.05)	27.1	52.1
Cup-to-disc area ratio	0.59 ± 0.21	0.45 ± 0.20	0.001	0.66 (0.05)	27.1	41.7
Horizontal cup-to-disc ratio	0.81 ± 0.19	0.72 ± 0.22	0.025	0.63 (0.05)	20.9	41.7
Cup volume, mm^3	0.34 ± 0.29	0.21 ± 0.20	0.016	0.63 (0.06)	12.5	37.5
Cup area, mm^2	1.07 ± 0.50	0.83 ± 0.46	0.017	0.62 (0.06)	22.9	33.3
Disc area, mm^2	1.73 ± 0.33	1.76 ± 0.35	0.682	0.51 (0.06)	8.3	22.9

* For comparison of mean values of ONH parameters between preperimetric glaucoma and control groups.

Investigative Ophthalmology & Visual Science

Downloaded from iovs.arvojournals.org on 03/01/2021

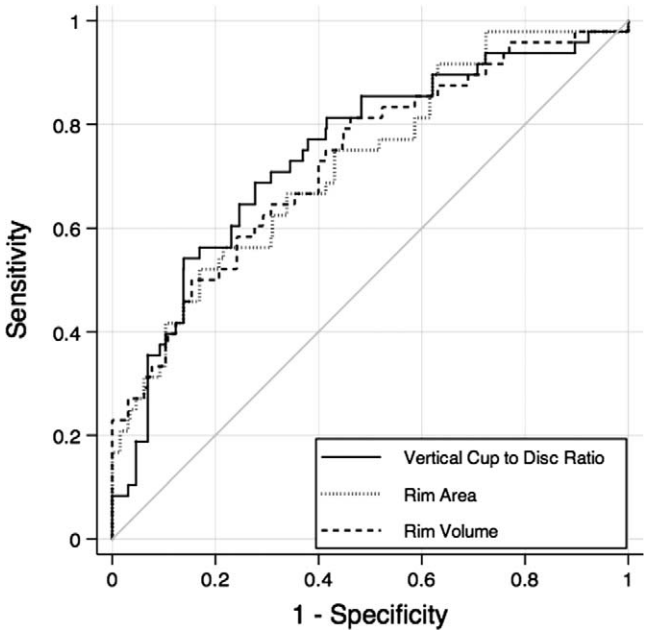

FIGURE 2. ROC curves the three ONH parameters with largest areas under the ROC curves: vertical cup-to-disc ratio, rim area, and rim volume.

as suspects in clinical practice (i.e., by clinical evaluation of photographs or fundoscopic examination at the slit-lamp). The worse performance of ONH compared with RNFL parameters could also reflect a weaker performance of the software in detecting topographic optic disc abnormalities. The ONH algorithm uses a reference line 150 μm above the RPE to define the transition between cup and rim, not taking into account individual variability, such as shallow or tilted optic discs. Moreover, although all images were reviewed, this protocol is still subject to human error, as manual delineation and centralization of the optic disc may be necessary. Conversely, the RNFL algorithm does not depend on a reference plane and may be less susceptible to the influence of normal phenotypic variations. However, it is important to keep in mind that, although ONH parameters performed worse than RNFL, it is possible that information provided by the ONH measurements could still potentially improve the diagnostic performance of the instrument if combined with that derived from RNFL assessment. For example, in a previous study by Medeiros et al.[20] that used the time-domain OCT, the authors showed that the combined information provided by different scanning areas had a better diagnostic accuracy than the information of each scan area separately. Further studies should investigate this hypothesis using SDOCT in a cohort of patients suspected of having glaucoma.

Since Zeimer et al.[5] first suggested that macular measurements could be useful for glaucoma diagnosis, several studies have been performed to test the effectiveness of such measurements in the detection of glaucomatous damage.[6,21–27] Theoretically, macular parameters have some advantages over RNFL parameters for glaucoma diagnosis. The macula has the highest concentration of ganglion cells in the retina and, therefore, loss of these cells could potentially be more readily detected at this region. Moreover, previous studies evaluating the time-domain OCT suggested that macular scans are more reproducible than RNFL scans.[28] This can be explained by the fact that RNFL scanning requires correct positioning of the scan circle by the operator and any misalignment tends to produce changes in RNFL measurements. Conversely, macular scans require internal fixation and are less dependent on the operator, which increases scan reproducibility.[29,30] Indeed, some studies showed that macular measurements are similar or even slightly better than RNFL measurements for glaucoma diagnosis.[22,25–27] However, our results did not show the same tendency, as RNFL measurements performed significantly better than macular measurements. The best macular parameter, GCC average thickness, had a considerably smaller AUC when compared with the best RNFL parameter. Moreover, in

TABLE 4. Mean ± SD Values of Macular Parameters With AUC Curves and Sensitivities at Fixed Specificities for Discriminating Between Preperimetric Glaucoma and Control Groups

Macular Parameters	Preperimetric Glaucoma, $n = 48$	Control, $n = 94$	*P* Value*	AUC (SE)	Sensitivity at 95% Specificity, %	Sensitivity at 80% Specificity, %
GCC parameters						
Average thickness, μm	83.6 ± 7.2	91.2 ± 6.6	<0.001	0.79 (0.04)	43.8	58.3
Inferior thickness, μm	83.0 ± 7.8	91.3 ± 6.8	<0.001	0.79 (0.05)	31.3	66.7
Superior thickness, μm	84.1 ± 7.5	91.1 ± 6.9	<0.001	0.76 (0.05)	31.3	62.5
Root mean square, %	0.10 ± 0.03	0.08 ± 0.02	<0.001	0.67 (0.05)	12.5	41.7
Global loss volume, %	11.3 ± 8.5	6.3 ± 5.1	0.002	0.65 (0.06)	33.3	58.3
Focal loss volume, %	1.9 ± 2.0	1.00 ± 1.2	0.011	0.59 (0.06)	14.6	43.8
S-I thickness, μm	1.1 ± 5.4	−0.2 ± 3.6	0.148	0.55 (0.05)	14.6	33.3
Full retinal parameters						
Inferior thickness, μm	250.4 ± 11.9	258.3 ± 13.6	0.004	0.70 (0.06)	8.3	45.8
Average thickness, μm	252.5 ± 11.7	260.2 ± 13.9	0.006	0.69 (0.06)	6.3	35.4
Superior thickness, μm	254.7 ± 12.3	262.1 ± 14.7	0.011	0.67 (0.06)	8.3	31.3
S-I thickness, μm	4.3 ± 5.7	3.8 ± 4.8	0.637	0.53 (0.05)	12.5	31.3
Outer retinal parameters						
S-I thickness, μm	3.2 ± 2.8	4.0 ± 2.8	0.151	0.58 (0.05)	10.4	37.5
Superior thickness, μm	170.6 ± 7.8	171.0 ± 10.5	0.828	0.53 (0.06)	0.0	12.5
Average thickness, μm	169.0 ± 7.6	169.0 ± 10.0	0.994	0.52 (0.06)	0.0	12.5
Inferior thickness, μm	167.4 ± 7.8	166.0 ± 9.8	0.830	0.50 (0.06)	0.0	12.5

S-I, superior minus inferior.
* For comparison of mean values of macular parameters between preperimetric glaucoma and control groups.

Investigative Ophthalmology & Visual Science

Downloaded from iovs.arvojournals.org on 03/01/2021

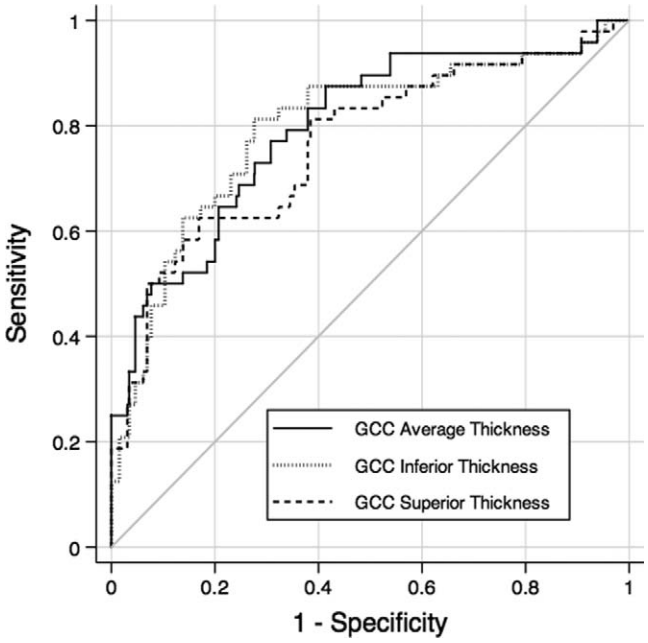

FIGURE 3. ROC curves for the three macular parameters with largest areas under the ROC curves: GCC average thickness, GCC inferior thickness, and GCC superior thickness.

Table 4 we can see that 6 of the 15 macular parameters were similar between preperimetric and control groups. It is also important to note that most of the studies that reported similar diagnostic performances between macular and RNFL parameters analyzed the SDOCT in a cohort of patients with more advanced stages of the disease. In advanced glaucoma, the macula has a higher chance of being involved and measurements at this region will probably be capable of detecting structural damage. Another possible explanation for the worse

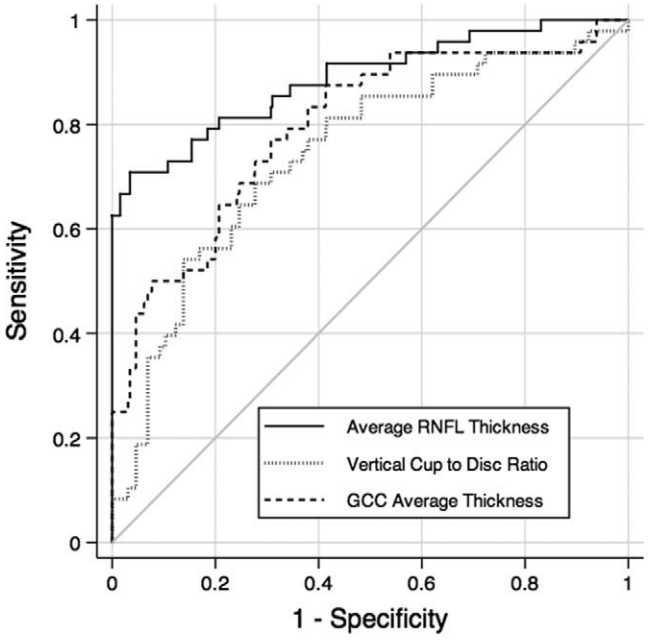

FIGURE 4. ROC curves for the parameters with largest AUCs of each protocol: inferior hemisphere RNFL thickness, vertical cup-to-disc ratio, and GCC retinal thickness.

performance of the GCC protocol is that the current algorithm available on the RTVue SDOCT does not differentiate the ganglion cell layer from the RNFL and internal limiting membrane. As nerve fibers from remote areas of the retina cross the area of macular scans, the ganglion cell layer thickness at a specific area might incorporate nerve fibers that do not correspond to the same affected area. It is possible that a segmentation algorithm that includes only the ganglion cell body layer could have better diagnostic performance than the one used in the current RTVue algorithm.

It is important to emphasize that the design used in our study evaluates only the situation of diagnosing preperimetric glaucoma in patients suspected of having the disease. Other study designs may be more relevant to evaluate the accuracy of SDOCT in other clinical scenarios. For example, if the study had the purpose of determining the ability of SDOCT to detect glaucomatous cases in situations of opportunistic screening, a design that contrasted patients with glaucoma versus unsuspected healthy eyes would have been more appropriate. Also, our design did not evaluate the ability of SDOCT to detect longitudinal changes. In fact, detection of progressive changes is usually the best way to clarify the diagnosis in eyes suspected of having glaucoma.[31] Further studies should evaluate the ability of the three scanning SDOCT areas to detect progressive damage in glaucoma suspects.

Longitudinal documentation of progressive disc damage was used in our study as the reference standard to obtain the final classification of eyes into cases and controls. Due to the wide variability of the optic disc appearances in the general population, a diagnosis of glaucoma cannot usually be made based on a single optic disc examination in eyes that do not show evidence of visual field loss. This study design enabled the evaluation of the performance of diagnostic tests in a scenario that resembles clinical practice and has been previously used in a similar situation.[11] However, it should be noted that this design might have some limitations. It might be argued that some patients from the control group could have developed glaucomatous optic disc damage or visual field defects after the end of the study and that the follow-up time was insufficient to detect them. Although it is unlikely that glaucoma patients would not progress or develop functional loss after having been followed untreated for almost 13 years, this possibility cannot be completely excluded. Another limitation of our study is that stereophotographic evaluation of the optic disc has an imperfect interobserver agreement.[32] As a consequence, some subjects could be misdiagnosed and incorrectly designated to the glaucomatous or to the control group. To minimize misclassifications, we required consensus grading by two expert ophthalmologists and a third experienced grader reviewed the stereophotographs in case of disagreement. Moreover, the use of progressive glaucomatous change as a reference standard requires longitudinal follow-up and serial documentation of the optic disc, which may not be available for all patients. Finally, difference in ancestry between groups was marginally significant in our study. Although previous studies reported that ancestry did not influence the diagnostic performance of the SDOCT technology,[33] we performed an additional analysis excluding black patients. As expected, similar results were achieved, with average RNFL thickness performing better than vertical cup-to-disc ratio (0.90 vs. 0.73; $P=0.009$) and GCC average thickness (0.90 vs. 0.80; $P=0.004$).

In conclusion, the results of this study demonstrated that SDOCT RNFL measurements performed significantly better than ONH and macular measurements in detecting preperimetric glaucomatous damage. Our results have significant implications for the use of the SDOCT technology for diagnosing structural damage in eyes suspected of having glaucoma. Future studies should evaluate whether a combina-

Investigative Ophthalmology & Visual Science

Downloaded from iovs.arvojournals.org on 03/01/2021

tion of different parameters can improve the performance of this technology to detect preperimetric glaucomatous damage.

Acknowledgments

Supported in part by National Institutes of Health/National Eye Institute Grants EY021818 (FAM), EY11008 (LMZ), and EY14267 (LMZ); Coordenação de Aperfeiçoamento de Pessoal de Nível Superior (CAPES) grant Bolsas no Exterior (BEX) 1066/11-0; an unrestricted grant from Research to Prevent Blindness (New York, New York); and grants for participants' glaucoma medications from Alcon, Allergan, Pfizer, Merck, and Santen.

Disclosure: **R. Lisboa**, None; **A. Paranhos Jr**, None; **R.N. Weinreb**, Alcon (C), Allergan (C), Bausch & Lomb (C), Carl Zeiss Meditec, Inc. (C), Nidek (S), Topcon (C), Aerie (S), Genentech (S); **L.M. Zangwill**, Carl Zeiss Meditec, Inc. (F), Heidelberg Engineering (F); **M.T. Leite**, None; **F.A. Medeiros**, Carl Zeiss Meditec, Inc. (F), Heidelberg Engineering (F)

References

1. Johnson CA, Sample PA, Zangwill LM, et al. Structure and function evaluation (SAFE): II. Comparison of optic disk and visual field characteristics. *Am J Ophthalmol*. 2003;135:148–154.
2. Johnson CA, Cioffi GA, Liebmann JR, Sample PA, Zangwill LM, Weinreb RN. The relationship between structural and functional alterations in glaucoma: a review. *Semin Ophthalmol*. 2000;15:221–233.
3. Harwerth RS, Carter-Dawson L, Smith EL III, Barnes G, Holt WF, Crawford ML. Neural losses correlated with visual losses in clinical perimetry. *Invest Ophthalmol Vis Sci*. 2004;45:3152–3160.
4. Medeiros FA, Zangwill LM, Bowd C, Mansouri K, Weinreb RN. The structure and function relationship in glaucoma: implications for detection of progression and measurement of rates of change. *Invest Ophthalmol Vis Sci*. 2012;53:6939–6946.
5. Zeimer R, Asrani S, Zou S, Quigley H, Jampel H. Quantitative detection of glaucomatous damage at the posterior pole by retinal thickness mapping. A pilot study. *Ophthalmology*. 1998;105:224–231.
6. Rao HL, Zangwill LM, Weinreb RN, Sample PA, Alencar LM, Medeiros FA. Comparison of different spectral domain optical coherence tomography scanning areas for glaucoma diagnosis. *Ophthalmology*. 2010;117:1692–1699, 1699.e1.
7. Leite MT, Rao HL, Zangwill LM, Weinreb RN, Medeiros FA. Comparison of the diagnostic accuracies of the Spectralis, Cirrus, and RTVue optical coherence tomography devices in glaucoma. *Ophthalmology*. 2011;118:1334–1339.
8. Park SB, Sung KR, Kang SY, Kim KR, Kook MS. Comparison of glaucoma diagnostic Capabilities of Cirrus HD and Stratus optical coherence tomography. *Arch Ophthalmol*. 2009;127:1603–1609.
9. Leung CK, Lam S, Weinreb RN, et al. Retinal nerve fiber layer imaging with spectral-domain optical coherence tomography: analysis of the retinal nerve fiber layer map for glaucoma detection. *Ophthalmology*. 2010;117:1684–1691.
10. Wang X, Li S, Fu J, et al. Comparative study of retinal nerve fibre layer measurement by RTVue OCT, GDx VCC. *Br J Ophthalmol*. 2011;95:509–513.
11. Medeiros FA, Zangwill LM, Bowd C, Sample PA, Weinreb RN. Use of progressive glaucomatous optic disk change as the reference standard for evaluation of diagnostic tests in glaucoma. *Am J Ophthalmol*. 2005;139:1010–1018.
12. Medeiros FA, Vizzeri G, Zangwill LM, Alencar LM, Sample PA, Weinreb RN. Comparison of retinal nerve fiber layer and optic disc imaging for diagnosing glaucoma in patients suspected of having the disease. *Ophthalmology*. 2008;115:1340–1346.
13. Medeiros FA. How should diagnostic tests be evaluated in glaucoma? *Br J Ophthalmol*. 2007;91:273–274.
14. Medeiros FA, Ng D, Zangwill LM, Sample PA, Bowd C, Weinreb RN. The effects of study design and spectrum bias on the evaluation of diagnostic accuracy of confocal scanning laser ophthalmoscopy in glaucoma. *Invest Ophthalmol Vis Sci*. 2007;48:214–222.
15. Lisboa R, Leite MT, Zangwill LM, Tafreshi A, Weinreb RN, Medeiros FA. Diagnosing preperimetric glaucoma with spectral domain optical coherence tomography. *Ophthalmology*. 2012;119:2261–2269.
16. Pepe M, Longton G, Janes H. Estimation and comparison of receiver operating characteristic curves. *Stata J*. 2009;9:1.
17. Zhou X-H, Obuchowski NA, McClish DK. Analysis of correlated ROC data. In: Zhou X-H, Obuchowski NA, McClish DK, eds. *Statistical Methods in Diagnostic Medicine*. New York: Wiley; 2002:274–306.
18. Alonzo TA, Pepe MS. Distribution-free ROC analysis using binary regression techniques. *Biostatistics*. 2002;3:421–432.
19. Rao HL, Kumbar T, Addepalli UK, et al. Effect of spectrum bias on the diagnostic accuracy of spectral-domain optical coherence tomography in glaucoma. *Invest Ophthalmol Vis Sci*. 2012;53:1058–1065.
20. Medeiros FA, Zangwill LM, Bowd C, Vessani RM, Susanna R Jr, Weinreb RN. Evaluation of retinal nerve fiber layer, optic nerve head, and macular thickness measurements for glaucoma detection using optical coherence tomography. *Am J Ophthalmol*. 2005;139:44–55.
21. Ojima T, Tanabe T, Hangai M, Yu S, Morishita S, Yoshimura N. Measurement of retinal nerve fiber layer thickness and macular volume for glaucoma detection using optical coherence tomography. *Jpn J Ophthalmol*. 2007;51:197–203.
22. Leung CK, Chan WM, Yung WH, et al. Comparison of macular and peripapillary measurements for the detection of glaucoma: an optical coherence tomography study. *Ophthalmology*. 2005;112:391–400.
23. Tan O, Li G, Lu AT, Varma R, Huang D. Mapping of macular substructures with optical coherence tomography for glaucoma diagnosis. *Ophthalmology*. 2008;115:949–956.
24. Ishikawa H, Stein DM, Wollstein G, Beaton S, Fujimoto JG, Schuman JS. Macular segmentation with optical coherence tomography. *Invest Ophthalmol Vis Sci*. 2005;46:2012–2017.
25. Moreno PA, Konno B, Lima VC, et al. Spectral-domain optical coherence tomography for early glaucoma assessment: analysis of macular ganglion cell complex versus peripapillary retinal nerve fiber layer. *Can J Ophthalmol*. 2011;46:543–547.
26. Seong M, Sung KR, Choi EH, et al. Macular and peripapillary retinal nerve fiber layer measurements by spectral domain optical coherence tomography in normal-tension glaucoma. *Invest Ophthalmol Vis Sci*. 2010;51:1446–1452.
27. Nakatani Y, Higashide T, Ohkubo S, Takeda H, Sugiyama K. Evaluation of macular thickness and peripapillary retinal nerve fiber layer thickness for detection of early glaucoma using spectral domain optical coherence tomography. *J Glaucoma*. 2011;20:252–259.
28. Gurses-Ozden R, Teng C, Vessani R, Zafar S, Liebmann JM, Ritch R. Macular and retinal nerve fiber layer thickness measurement reproducibility using optical coherence tomography (OCT-3). *J Glaucoma*. 2004;13:238–244.
29. Vizzeri G, Bowd C, Medeiros FA, Weinreb RN, Zangwill LM. Effect of signal strength and improper alignment on the variability of stratus optical coherence tomography retinal nerve fiber layer thickness measurements. *Am J Ophthalmol*. 2009;148:249–255.e1.
30. Schuman JS, Pedut-Kloizman T, Hertzmark E, et al. Reproducibility of nerve fiber layer thickness measurements using optical coherence tomography. *Ophthalmology*. 1996;103:1889–1898.

Investigative Ophthalmology & Visual Science

Downloaded from iovs.arvojournals.org on 03/01/2021

31. Medeiros FA, Alencar LM, Zangwill LM, Bowd C, Sample PA, Weinreb RN. Prediction of functional loss in glaucoma from progressive optic disc damage. *Arch Ophthalmol*. 2009;127:1250–1256.
32. Breusegem C, Fieuws S, Stalmans I, Zeyen T. Agreement and accuracy of non-expert ophthalmologists in assessing glaucomatous changes in serial stereo optic disc photographs. *Ophthalmology*. 2011;118:742–746.
33. Girkin CA, Liebmann J, Fingeret M, Greenfield DS, Medeiros F. The effects of race, optic disc area, age, and disease severity on the diagnostic performance of spectral-domain optical coherence tomography. *Invest Ophthalmol Vis Sci*. 2011;52:6148–6153.

Investigative Ophthalmology & Visual Science

Downloaded from iovs.arvojournals.org on 03/01/2021